International Conference on Space Optics—ICSO 2022

Dubrovnik, Croatia

3–7 October 2022

Edited by Kyriaki Minoglou, Nikos Karafolas, and Bruno Cugny,

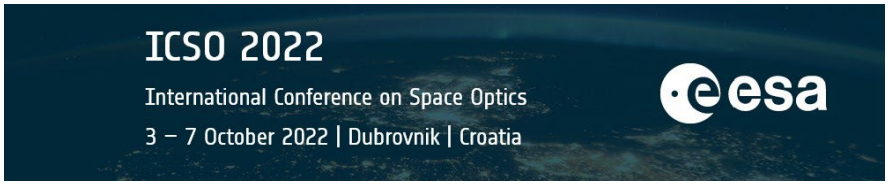

Pyroelectric Detector for EE9 FORUM: Design and Characterization

International Conference on Space Optics — ICSO 2022, edited by Kyriaki Minoglou, Nikos Karafolas, Bruno Cugny, Proc. of SPIE Vol. 12777, 127773Q · © 2023 ESA and CNES · 0277-786X · doi: 10.1117/12.2690559

Pyroelectric Detector for EE9 FORUM: Design and Characterization

A. Neuzner*[a], A. Hacker[a], L. Pérez Prieto[a], R. Mistry[b], M. Zahir[c]
[a]Airbus Defence and Space GmbH, Robert-Koch Str. 1, 82024 Taufkirchen (D)
[b]Leonardo UK, First Avenue Southampton, SO15OLG (UK)
[c]European Space Agency TEC/MME, Keplerlaan 1, 2200 Noordwijk (NL)

ABSTRACT

The **F**ORUM **S**ounding **I**nstrument (FSI) is a step-and-stare Fourier-transform infrared spectrometer that performs radiometry on light leaving the earth within a spectral range from 6.25 to 100 µm. During the scan of the pendulum-type interferometer, the light intensity at the two output ports is recorded by a detection chain based on modified component-off-the-shelf pyroelectric detectors. This paper reports on fundamental detector properties and the results of electro-optical characterization. In contrast to the majority of established literature, the characterization was performed using visible light permitting a high degree of control over geometric and modulation properties of the optical stimulus. The results significantly contributed to a thorough understanding of the detector and the choice of the best design for the FORUM mission. This paper represents the status of the work at the start of project phase B2.

Keywords: FORUM, FTIR, Pyroelectric Detectors, Thermal detection, DLATGS, (V)LWIR

1. MISSION CONTEXT AND INSTRUMENT

The ***F**ar-Infrared **O**utgoing **R**adiation **U**nderstanding and **M**onitoring* (FORUM) mission is ESA's 9th *Earth Explorer* [1] due to be launched in 2027. The space segment hosts two optical instruments. The main instrument (FSI) is a pendulum interferometer that performs spectrally resolved radiometry on light leaving the earth within a spectral range of 6.25 to 100 µm. The instrument operates in a step-and-stare mode; each sample contains information on light originating from a ground sample of 15 km in diameter per 100 km step. It is accompanied by the ***FORUM E**mbedded **I**mager* (FEI), a thermal imager based on a bolometric array as secondary instrument.

The light collected at the FSI entrance aperture is split into equal halves by a Germanium-coated diamond beam splitter. The two fields are recombined on a second beam splitter after having traversed different optical paths. The light intensity at the two output ports depends on the optical phase difference and hence on the light wavelength and the optical path difference. While the scanning mirror tracks a ground element, the interferometer continuously scans the optical path difference at a rate of 0.2 cm/s. Each monochromatic constituent of the collected light field is thereby mapped onto a characteristic intensity modulation frequency at the interferometer output. The input optical spectral range of 6.25-100 µm is mapped onto an output intensity modulation frequency range of 19-320 Hz. The light leaving the two output ports is imaged by the ***B**ack-**T**elescope and **D**etection **A**ssembly* (BTDA) onto a single detector element. A record of the light intensity as a function of the optical path difference allows to reconstruct the spectrum of the incident light.

The mission has recently entered phase B2/C/D with *Airbus Stevenage* acting as mission prime contractor and satellite integrator. The FSI instrument is being developed by *OHB System AG in Oberpfaffenhofen* and the BTDA including the pyroelectric detection chain is developed, built and characterized under responsibility of *Airbus Ottobrunn*.

The mission context generates a series of rather untypical requirements and peculiarities for the detection chain of the FSI:

- The broad spectral coverage including the VLWIR range up to 100 µm rules out the usage of quantum detectors.
- The broad spectral range further narrows the choice of optical materials. Common crystaline infrared materials like ZnSe or CsI are opaque at 100 µm. Typical THz materials on the other side are not yet transparent at 6.25 µm. The few transmissive elements in the optical system – including the detector entrance window – are made from diamond.

* andreas.neuzner@airbus.com; Phone: +49-89 3179 8190

- The modulation frequency range up to 320 Hz requires a detector with time constant that is short for thermal detectors.
- The FTIR instrument principle requires good knowledge of the amplitude and phase transfer function of the detection system. Further the spectral gradients of amplitude and phase need to be limited in order to prevent the generation of spectral sideband modulation as a consequence of interferometer speed instabilities.
- In contrast to discretized imaging systems, the relevant noise figure is not the total RMS noise at the output of the detection chain but the frequency-resolved noise spectral density within the relevant band of 19-320 Hz.
- The detector sits at a pupil of the instrument optical layout. This is to ensure that spatial inhomogeneities of the detector do not translate into inhomogeneities of on-ground sensitivity. The optical system necessitates a lens with very short focal length in close vicinity of the detector sensitive element. This is realized by the usage of a plano-convex diamond lens as detector entrance window.

The BTDA is based on a Series 106 pyroelectric detector from Leonardo UK as a modified component off-the-shelf. Leonardo has been producing high-performance pyroelectric detectors based on **d**euterated **L**-Alanine doped **t**ri-**g**lycine **s**ulfate (DLATGS) for many years in large quantities. The detectors are used e.g. in FTIR laboratory equipment for chemical analysis. Series 106 detectors were previously flown in several space missions including the Mars Exploration Rovers Spirit and Opportunity, Osiris-Rex and Phobos-Grunt and are foreseen for Lucy and Clarreo [2]. All these missions use standard Series 106 detectors in TO5 housings with slight modifications to the geometry and the entrance window. FORUM as well will make use of a custom, precision-machined TO5 housing to adapt the window-to-detector distance and will further use a diamond lens as entrance window where Leonardo within the COTS design uses flat windows.

This paper reports on measurements done on two Series 106 detectors that were done in the context of a detector breadboarding activity carried out at Airbus at the start of Phase B2. The goal of this campaign was to get a better understanding of the underlying detector physics in order to make an educated choice between several subtle design variants within the Series 106 detectors. Further, earlier measurements in Phase A/B1 had concluded partially inconclusive results and the campaign was aimed to clarify some of the questions posed. This especially pertains to the necessity of using instrument-representative, i.e. spot illumination for detector performance characterization.

2. PYROELECTRIC DETECTION

Pyroelectricity is the property of certain crystal systems to generate charge displacement in response to changes in temperature. This effect has been known since ancient times and has been exploited to build detectors since the mid 20th century. Pyroelectric detectors are intrinsically thermal detectors. Incident radiation of all types is converted to heat by the means of a suitable absorber. The absorbed heat causes a rise in temperature of the detector crystal which via the pyroelectric effect causes a charge to be deposited on the crystal surfaces. Electrodes that are deposited on the crystal pick up the charge and a resulting current flow between the two crystal facets creates a detectable signal (see Figure 2-1).

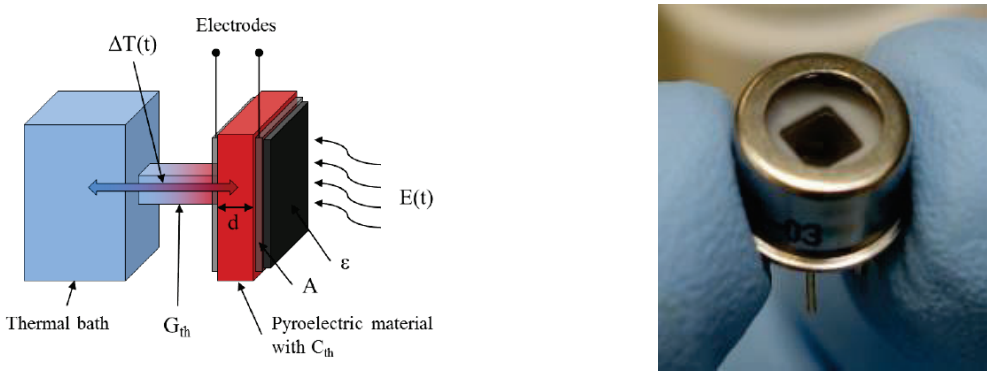

Figure 2-1 Left: Functional sketch of a pyroelectric detector. The sketch does not show the shunt resistor and JFET that are included in the detector package (see text). Right: Photography of the Leonardo P5625 Series 106 detector with flat CsI window that was used in the reported study.

A simple performance model can be setup by simplifying the thermal part of the model to a single thermal node. The model presented here is documented in literature [3], [4]. Leonardo UK works with an extended model that is accessible to Airbus but is company proprietary – as are detector design and material specific quantities – and cannot be quoted here.

The simplified model is shown in Figure 2-2. The left part shows an equivalent thermal circuit with heat capacity $C_{th}(J/K)$ and a thermal link with conductivity $G_H(W/K)$ to an ambient heat bath. The temperature response with respect to modulations of the incident power has a low-pass behavior with a cut-off frequency at $f_{th} = (2\pi\tau_{th})^{-1}$ with the thermal time constant $\tau_{th} = C_{th}/G_H$. At very low frequencies, the temperature of the crystal directly follows the applied input power including constantly applied power that will lead to a constant temperature increase in steady state. At modulation frequencies significantly above the thermal cut-off frequency, the crystal temperature response $T(t)$ will decrease with 1/f with the applied modulation frequency and acquire a 90° phase shift. The FORUM detector has a typical value for τ_{th} of 140 ms and the FORUM modulation frequency range thus lies far above the thermal cut-off frequency of 1.13 Hz.

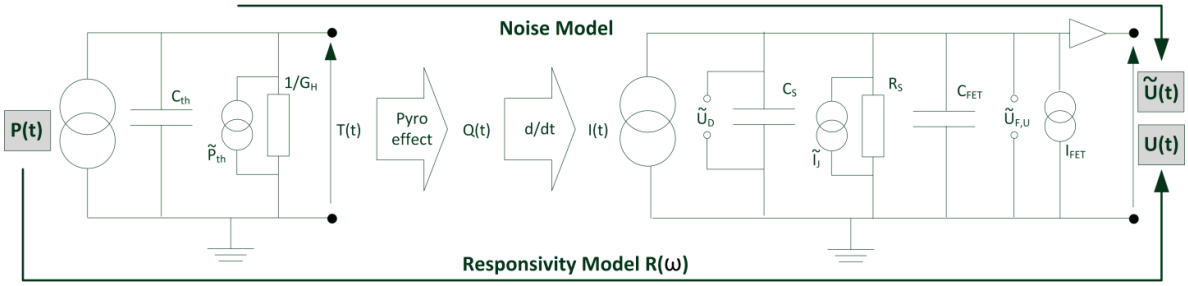

Figure 2-2 Structure of the thermal and electrical detector performance model. Quantities with tildes indicate noise sources.

The pyroelectric effect will result in a charge $Q(t) = p \cdot A \cdot T(t)$ being deposited on the crystal facets proportional to the temperature, crystal surface A and specific pyroelectric coefficient p $(C/m^2/K)$. The resulting current that flows through an electrical connection between the two electrodes is $I(t) = dQ(t)/dt$. The derivation with respect to time compensates the 1/f behavior of the temperature response and leads to a constant current response of the detector above the thermal cut-off temperature. This is shown quantitatively in Figure 2-3 for detector parameters that are close to the detector baselined for FORUM in response to an input power of 120 µWpp. It shall be mentioned that this model considers only conductive loss channels in which the heat loss is proportional to the temperature difference between crystal and ambient heat bath. Radiative losses scale with the fourth power of the crystal temperature and are hence intrinsically non-linear. For operation at ambient temperatures and within the relevant FORUM parameter space this is however a negligible effect (numeric analysis shows that less than 1% of the thermal power is lost due to radiation even when operating the detector at maximum input power relevant for FORUM).

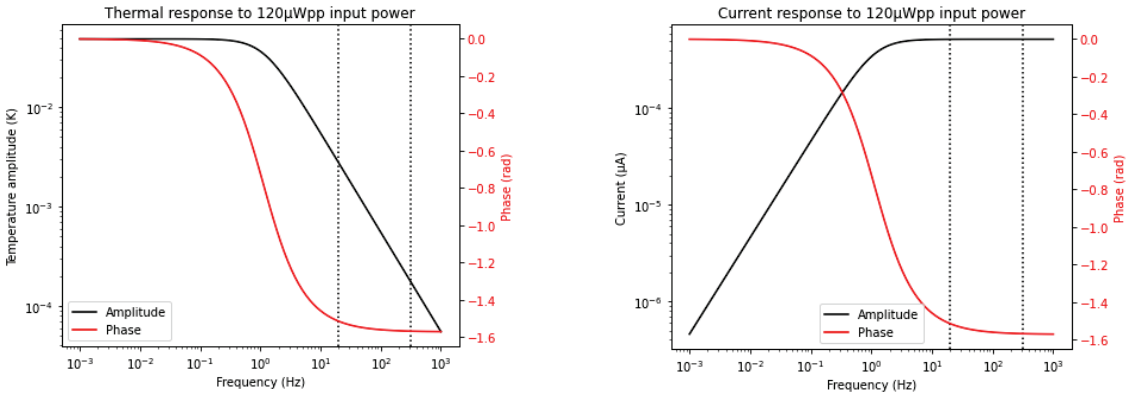

Figure 2-3 Simulated thermal response (left) and current response (right) caused by 120 µWpp input power for a detector that is very similar to the baselined FORUM detector in response to a 120 µW peak-to-peak absorbed optical power as a function of the modulation frequency. The dashed vertical lines indicate the FORUM operating range. Note that the phase of the current response is calculated w.r.t. a different reference and misses an additional 90° offset.

In the FORUM design, an additional high-impedant (>10 GOhm) shunt resistor (R_S *in* Figure 2-2) is inserted into the electrical connection between the two electrodes to convert the modulated pyroelectric current into a voltage signal. A junction field-effect transistor (JFET) electrically separates the high-impedant detector internal circuit from external detection chain circuitry. The shunt resistor together with the electrical capacity of the electrodes deposited on the crystal C_S and junction capacity of the JFET C_{FET} adds an additional high-pass transfer function to the system in the conversion of charge to volts with a cut-off frequency of $f_{el} = [2\pi R_S(C_S + C_{FET})]^{-1}$. For the FORUM detectors, this frequency is on the order of 10 mHz.

The resulting end-to-end transfer gain in units of V/W_{abs}, i.e. output voltage per absorbed optical power is shown in Figure 2-4 together with the predicted phase. These simulations were done using Leonardo proprietary parameters on a design that conforms with the Leonardo Series 106 COTS design and has a sensitive surface area of 3.14 mm². The FORUM modulation frequency range (indicated by the black dotted lines) is almost a complete order of magnitude above the thermal cut-off frequency and thus an almost perfect 1/f behavior of the detector responsivity is expected. An important property of the detector is that it is intrinsically AC coupled. Signals that are modulated slower than the electrical cut-off frequency are strongly suppressed. DC power input will cause a constant increase of the crystal temperature but the resulting pyroelectric charge will quickly be compensated by a transient current through the shunt resistor and no steady-state output signal will be caused. This has strong repercussions on detector- and instrument-level test philosophy as the detector is blind to unmodulated light stimuli.

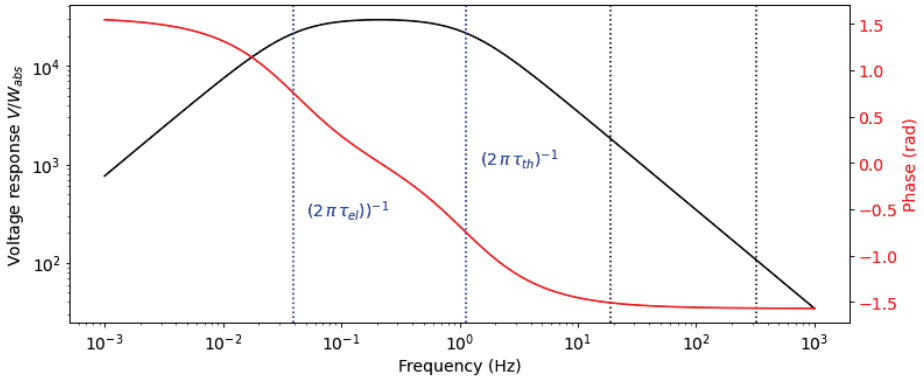

Figure 2-4 Simulated voltage response of a FORUM-type Leonardo pyroelectric detector with sensitive area of 3.14 mm². The black dashed lines indicate the FORUM spectral range. The dashed blue lines indicate the two relevant corner frequencies, i.e. the electrical and thermal cut-off frequencies.

The quantities with tildes in Figure 2-2 represent noise sources within the detector. The relevant noise terms are

- Johnson noise of the shunt resistor
- Schottky noise of the JFET leakage current
- Thermal Johnson noise of the conductive heat link to the ambient bath
- JFET voltage noise
- Dielectric noise ($\tan(\delta)$-noise) due to electrical loss mechanisms within the detector

Most individual noise constituents have white noise spectrum but when propagated to the detector output, they experience different spectral weighting and the output noise spectrum is thus not white. The simulated total noise spectral density for the same Leonardo S106 detector parametrization that was used in the simulation of the responsivity above is shown in the left panel of Figure 2-5. The right panel of Figure 2-5 shows simulated output voltage noise equivalent absorbed optical power spectral density. This quantity is calculated by dividing the noise spectral density by the responsivity. This quantity describes an effective noise source in Watts/sqrt(Hz) that when put in front of a noiseless detector would result in the same output noise as the real detector.

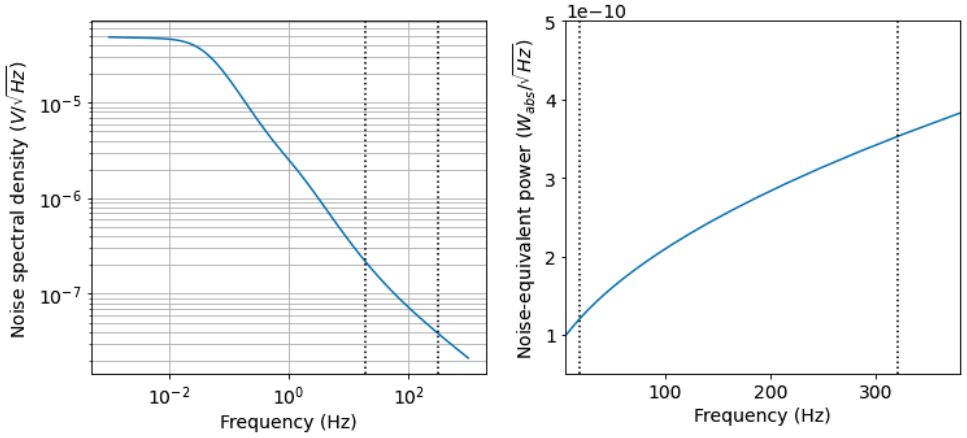

Figure 2-5. Left: Simulated total output voltage noise spectral density; Right: Simulated noise-equivalent absorbed optical power. Simulations are performed for a FORUM-type Leonardo pyroelectric detector with a sensitive area of 3.14 mm². The dashed lines indicate the FORUM modulation frequency range.

3. CHARACTERIZATION SETUP

Historically, long-wave infrared detectors are characterized using chopped blackbody sources. These reliably provide low-noise long-wave infrared radiation with well-known radiometry. However, when putting the detector directly in front of the source, it will intrinsically be flat-field illuminated. A potential problem arises here as the detector itself becomes the radiometrically relevant aperture. In order to calculate responsivity "*output signal per input power*", the input optical power needs to be calculated by multiplying the flat-field input intensity with the detector sensitive area size. Errors in the knowledge of the sensitive area size thus directly lead to errors in the evaluated responsivity. In FORUM however - as in most FTIR applications - a light spot with finite size will be cast to within the sensitive area.

When using a small aperture and a relay optics on a blackbody to generate spot illumination, the available power is very much limited and the radiometry is significantly complicated. Further, the chopping will ideally provide a rectangular modulation of the light beam in the case where the beam is very small compared to the apertures in the wheel. In a typical situation – e.g. where the chopper sits directly in front of a spatially extended blackbody aperture or cuts through a beam with finite extent and inhomogeneous profile – the intensity trajectory will be more complicated. Assumptions have to be made to calculate the amplitude of the fundamental chopping frequency from the chopping geometry. Also, FORUM will require very good knowledge of the transfer phase of the detector. This leads to a knowledge requirement on the timing of the chopper in the order of µs which is hardly feasible on a mechanical system.

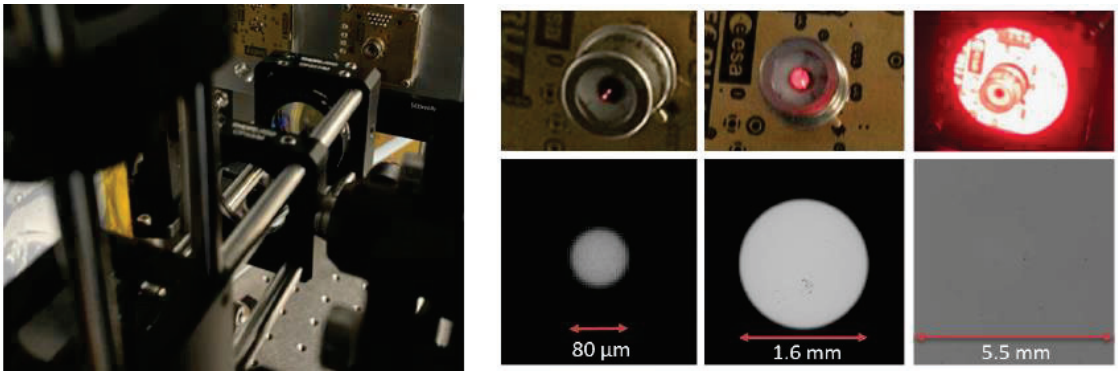

Figure 3-1 Left: Picture of the characterization setup positioned in front of a detector mounted onto the proximity electronics. Right: photographies and beam profiles of the three different realized illumination geometries – from left to right: 80 µm spot configuration used for measurements of spatial homogeneity, 1.6 mm spot configuration used as FORUM-representative illumination and flat-field illumination.

For the abovementioned reasons, we decided to use a VIS light source based on a high-power LED at 650 nm with direct modulation of the drive current. The thermal detection mechanism itself is per se agnostic on the used wavelength. While differences in optical properties of the used window materials and the black coating between the characterization wavelength and the usage wavelength are relevant for absolute radiometry, these are well-known and typically small. Also these only affect absolute radiometry and not quantities like relative amplitude differences e.g. between different illumination positions or frequencies and phase transfer.

The optical setup is sketched in Figure 3-2. The light is coupled into a multi-mode fiber and led to an optical setup built from *Thorlabs* cage system. The entire setup is mounted onto a three-axis translation stage. The light leaving the fiber is collimated and a 90:10 beam splitter taps off a constant fraction of the light that is imaged onto a reference photodiode. This photodiode has a bandwidth of 90 kHz that is high compared to FORUM relevant frequencies and thus provides a reliable in-situ measurement of the modulated light output. Light that passes the beam splitter is refocused and imaged onto the detector under test. This system thus creates an incoherent image of the end facet of the multimode fiber on the detector. Three different configurations were used that differ in the fiber core diameter and the lens focal lengths and resulted in illuminated disks on the detector with diameters of 80 µm, 1.6 mm and flat-field illumination. A calibrated optical power meter and a CMOS camera used as beam profiler can be inserted into the beam instead of the device under test. Verification measurements on the setup were performed to characterize the amplitude and phase transfer functions of the system as well as its linearity. The setup is typically operated with a CW offset of 50 µW and a modulated peak-to-peak power of 40 µW. Thus, the potentially non-linear very-low power regime of the LED is avoided. The CW offset does not affect the measurements since the detector is intrinsically AC coupled and the CW light field simply leads to a constant but very small raise in crystal temperature.

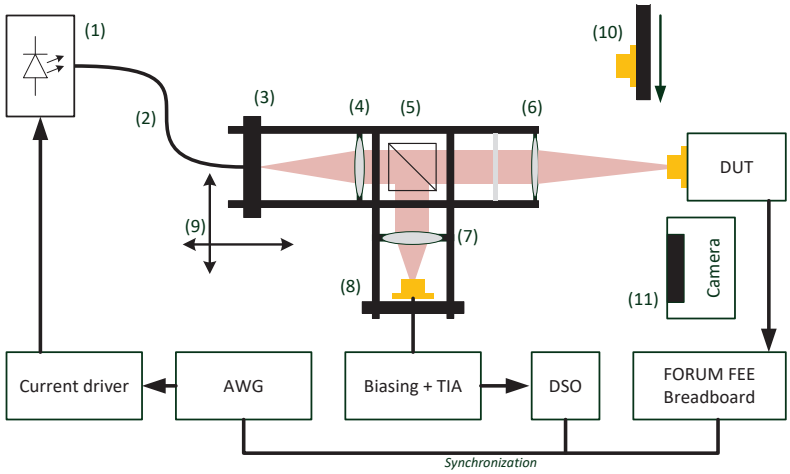

Figure 3-2: Sketch of the optical setup. (1) High –power LED, (2) Multi-mode fiber, (3) cage system (4) collimating lens, (5) 90:10 beam splitter, (6) focusing lens, (7) focusing lens for reference diode (8) reference diode, (9) Three-axis translation stage,(10) calibrated optical power meter, (11) CMOS camera; The abbreviations denote Arbitrary Wave Generator (AWG), Trans-Impedance Amplifier (TIA), Digital Storage Oscilloscope (DSO), Front-End Electronics (FEE) and Device-under-test (DUT)

In order to operate the detectors, Airbus Toulouse has designed a detection chain breadboard during FORUM Phase A/B1. The detection chain breadboard implements a split between a proximity electronics and a front-end electronics. The detector is mounted onto a socket of the proximity electronics and is connected such that its-internal JFET is operated self-biased as a source follower. The downstream electronics contains a complex analog filter that attempts to flatten the complete system response by compensating the detector-intrinsic 1/f behavior of responsivity with a rising slope in electrical response function. In the context of this study, the detection chain breadboard is used as an EGSE to perform measurements on the detectors. Only detector-related properties are reported. To allow for this, a characterization of the electrical response function of the breadboard was done during GSE commissioning of this study.

4. CHARACTERIZATION RESULTS

Devices under test

A large number of Series 106 and Series 99 detectors from Leonardo UK were characterized using chopped blackbody illumination during FORUM Phase A/B1. The campaign reported herein was conducted to address some open questions and solve inconsistencies within the data gathered in Phase A/B1. To this end, two Series 106 detectors were tested that differ in the electrode geometry – see Figure 4-1. In both designs, the actual pyroelectric crystal is significantly larger than the nominal sensitive area. The sensitive area is given by the overlap region between the two electrodes deposited on the top and the bottom of the crystal. It is only within this region that pyroelectric displacement within the crystal has a finite projection onto the electric field of the capacitor formed by the two electrodes and hence leads to net charge transfer. Light that impinges outside of this area will only lead to a local displacement of charges on one of the two electrodes without detectable net charge transfer. The two detectors under test differ in the design of the electrodes and how the overlap region is formed.

In the round design (P5625), two concentric, round electrodes are put onto the two sides of the crystal and the nominal sensitive area – which is the overlap area of the two electrodes – is defined by the size of the lower electrode which is smaller than the upper one. An electrical connection to the lower electrode hence necessarily needs to sit within the sensitive area. In the rectangular design (P5313), the sensitive area is formed as the intersection area of two elongated stripes that intersect at 90°. In this design, the electrical connections to the electrodes can be done outside of the nominal sensitive area.

The P5625 has a nominal sensitive area size of 2 mm diameter. The P5313 rectangular design has a nominal area size of 2x2 mm². The rectangular detector design is baselined for FORUM.

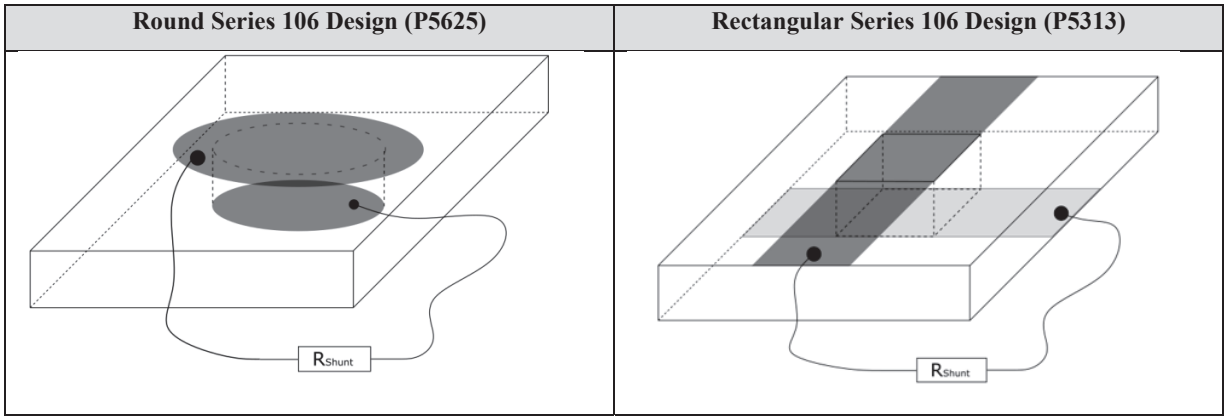

Figure 4-1 Round (left) and rectangular (right) electrode configuration. The sketches show the crystal disk and the electrodes deposited on the two sides. The sensitive crystal volume enclosed within the overlap area of the two electrode is indicated with dashed lines. Note that an additional black spot that is deposited on top of the crystal to enhance optical absorptivity is not shown in the sketch.

Spatial homogeneity and sensitive area geometry

The optical setup was configured to project an 80µm spot onto the detector. The light was modulated at 19, 78, 158 and 320 Hz and scanned in steps of 80 µm over an area of 8x8 mm². At each position, the resulting detector signal was recorded and spatial maps of responsivity were calculated.

The data recorded on the round P5625 is shown in Figure 4-2. At 320 Hz, one can clearly recognize the sensitive surface with 2mm diameter. The responsivity within the sensitive surface shows good homogeneity with approximately 5% local variations. When decreasing the modulation frequency, a local drop in responsivity appears within the upper left quadrant of the sensitive surface. At the lower end of the FORUM relevant frequency range, 19 Hz, the responsivity drops to almost zero in the center of this feature. The origin of this feature lies within the thermal part of the detector model. The model discussed above is oversimplified in that it used a single thermal node with a scalar heat capacity, temperature and a single thermal link to the environment. In reality the modulated light beam will cause a three-dimensionally extent temperature field in the bulk of the crystal that consists of a constant part and an oscillating part. The penetration depth of the oscillating

part scales with the modulation frequency. At very high frequencies, only the temperature at the crystal surfaces is modulated whereas low temperatures will modulate the bulk crystal. Therefore at low temperatures, the thermal model will respond to thermal properties of the crystal rear surface. This is known from literature [6],[7],[8]. In case of the P5625 detector, the observed feature stems from structures on the rear surface used to electrically connect the rear electrode. A similar effect has been reported in a characterization of a Leonardo Series 99 detector done by NPL [8].

Typically, these detectors are operated at higher frequencies. The very long wavelength relevant for FORUM however leads to very low minimum modulation frequencies at which heat-sinking features start to appear. For the instrument, such a feature may become problematic in that properties of the overall signal chain will depend on the exact position of the light spot within the sensitive surface and its spatial overlap with the heat-sinking feature. Further, characterization data gathered with flat-field illumination will not show performance that will be observed similarly with spot illumination.

The P5625 data further shows responsivity appearing outside of the nominal sensitive area at low modulation frequencies. The excess responsivity is not very high but the affected area is in total comparable to the nominal sensitive area. The detector will thus show stronger response under flat-field illumination as the effective sensitive surface size grows at low frequencies. The origin of this effect is unclear.

The data recorded on the rectangular P5313 is shown in Figure 4-3. It does not show heat-sinking features similar to the P5625. As discussed above, the rectangular design allows to electrically contact the electrodes on both sides of the crystal outside of the sensitive area. In fact, a small feature can be seen on the upper left edge in the plot at low modulation frequencies. This feature is caused by the contact to the lower electrode similar which however sits outside of the sensitive area and under the optically opaque crystal carrier structure. The P5313 electrode stripes are both 2 mm wide and one would thus expect a 2x2 mm² sensitive surface. The measured sensitive surface however has a size of 2x3 mm². This is a consequence of the black coating that is put on top of the crystal that is electrically conductive itself. It thus effectively enlarges the upper electrode. One should be aware that the internal electrical impedance is extremely high and thus already a small conductivity of the black coating is sufficient to cause this effect. When performing flat-field illuminated measurements, accurate knowledge of the sensitive surface size is required. Assuming a 2x2 mm² sensitive surface as suggested by the electrode configuration alone would lead to an overestimation of 50% of the detector responsivity.

Both datasets further show that the detector responsivity does not drop completely to zero even far outside of the nominal sensitive region. This is a common effect observed also in photodiodes packed in TO housings. Reflections inside of the TO housing create rogue light paths via which signal is caused on the detector even if the source of the illumination is far outside the nominal sensitive area. The relevance of these effects depend on the detector use case. When the detector is used to measure intensity in a flat-field illuminated setup, the rogue light paths simply add to the signal and need to be taken into account for detector calibration. If however the detector is characterized with flat-field illumination and later used with spot illumination, the flat-field measurement will overestimate the relevant spot-illuminated responsivity.

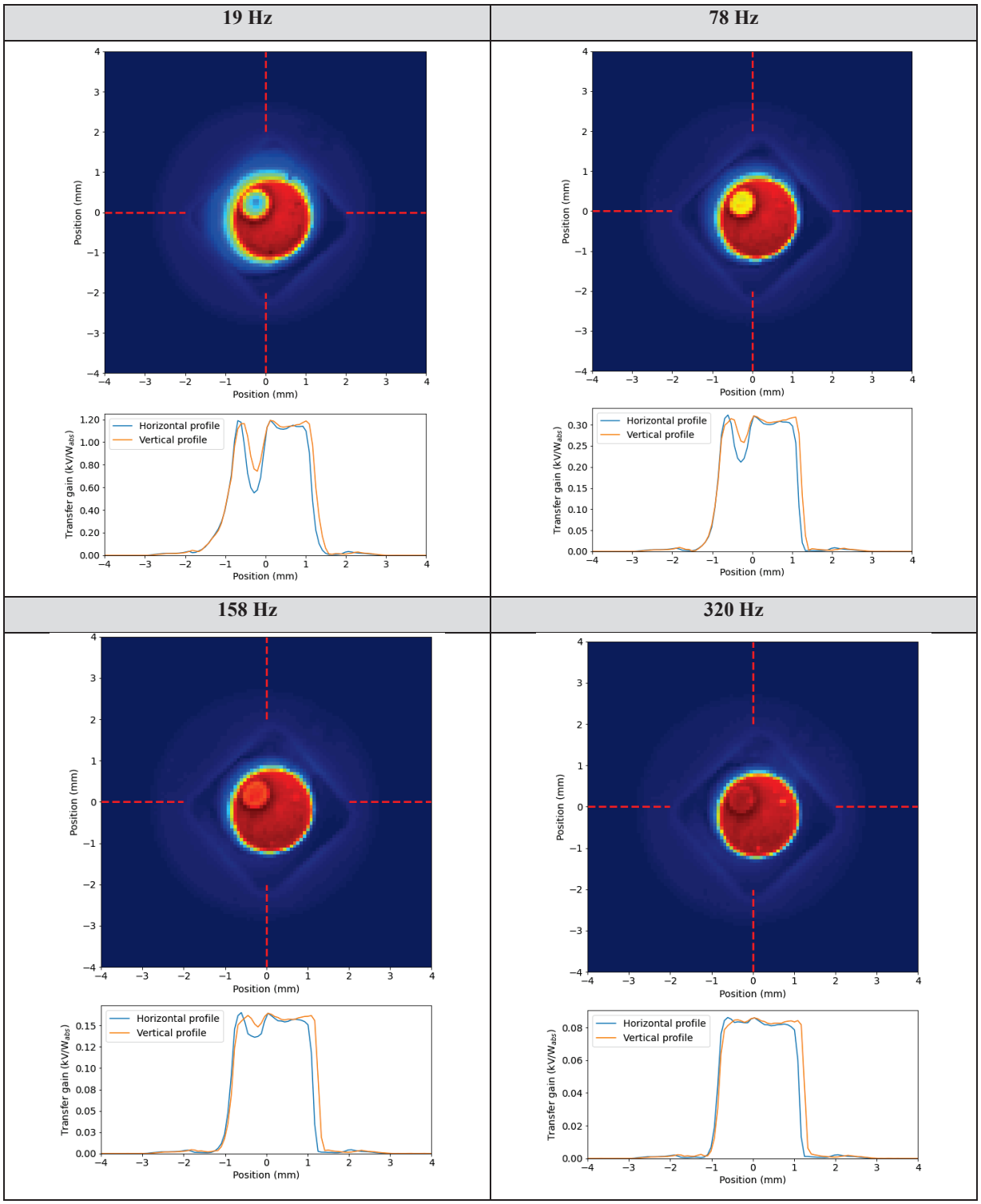

Figure 4-2: Spatial maps of responsivity (Volts per Watt absorbed optical power) as recorded on the P5625 detector with round sensitive surface. Data was recorded at four different modulation frequencies. Note that the color code on the spatial maps is normalized to the peak responsivity whereas the axis on the data profiles show the absolute values.

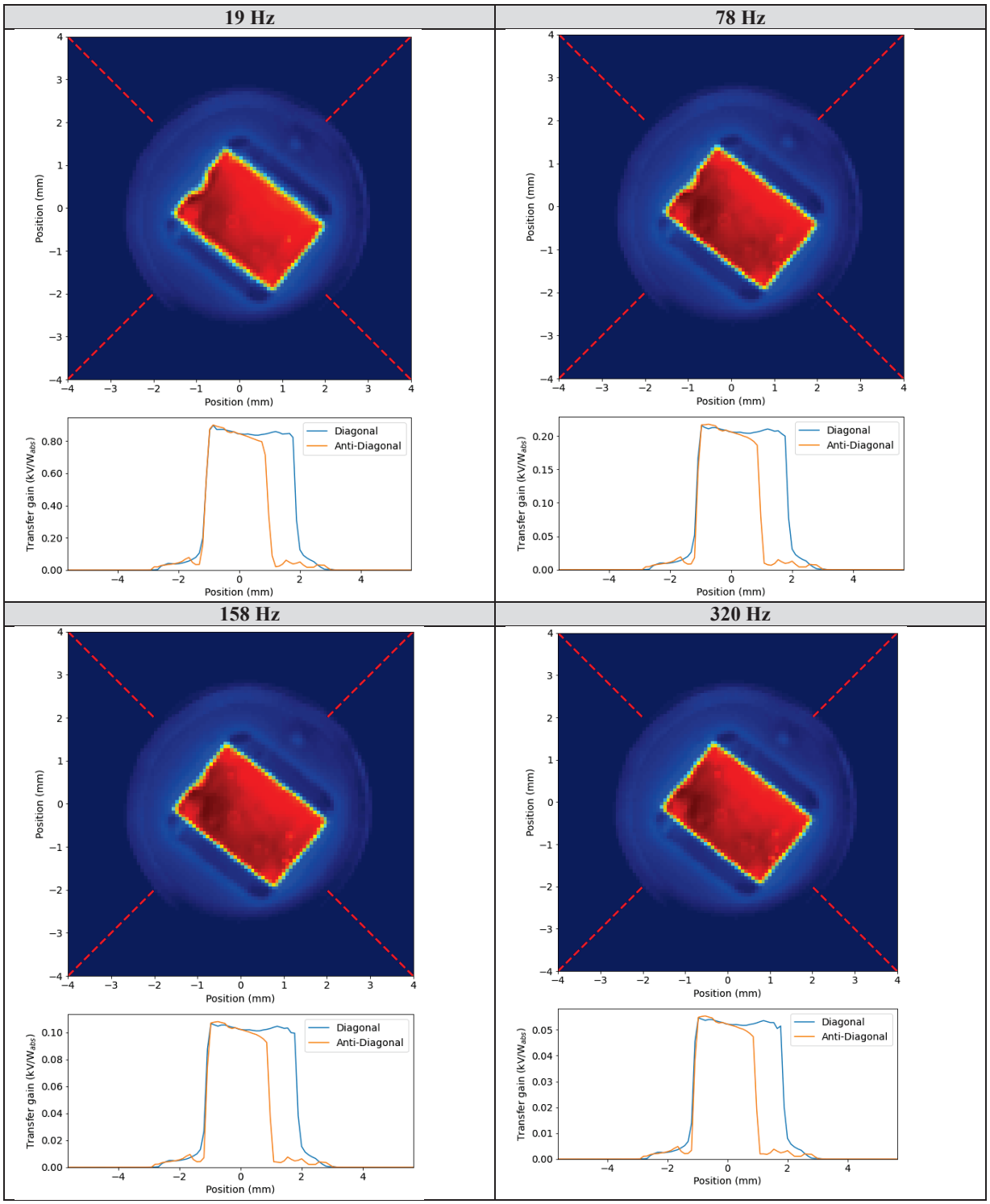

Figure 4-3: Spatial maps of responsivity (Volts per Watt absorbed optical power) as recorded on the P5313 detector with rectangular sensitive surface. Data was recorded at four different modulation frequencies. Note that the color code on the spatial maps is normalized to the peak responsivity whereas the axis on the data profiles show the absolute values.

Transfer function and noise-equivalent power

The detector transfer function amplitude and phase has been measured using the optical setup to project a large spot (1.6 mm diameter) onto the detector and also using flat-field illumination. The spot illumination is similar to the FORUM optical setup in size and in the fact that the spot is smaller than the detector sensitive surface. The flat-field illumination was done to allow for consistency checks with earlier measurements. It had been assumed that some discrepancies that appeared in Phase A/B1 could be explained this way. The input power in the spot-illuminated case was measured directly by impinging the complete beam on a calibrated optical power meter. In case of the flat-field illuminated case, the input power was calculated by measuring the intensity of the homogeneous illumination (using the same calibrated optical power meter with an aperture of known size in front of it) and multiplying it with the 2x3 mm² detector size. Note that here we are using the measured value of the detector size as opposed to the nominal value of 2x2 mm². All data sets were corrected for losses on the optical input windows and finite coating absorption and the values are thus applicable to absorbed optical power. The phase evaluation was done relative to the phase as measured by the reference photodiode in the optical setup and removing the previously measured phase shift caused by the electronic signal chain.

The measurement results for the round P5625 and the rectangular P5313 detector are shown in Figure 4-4. The black lines in both plots indicate the predictions of the performance model. One should keep in mind that the Leonardo performance model predicts *typical values* and a significant device-to-device variation in performance exists. The data shows that flat-field illumination concludes a higher responsivity than spot-illumination. As discussed above this is likely a consequence of rogue light paths and potential uncertainty in the size of the sensitive area.

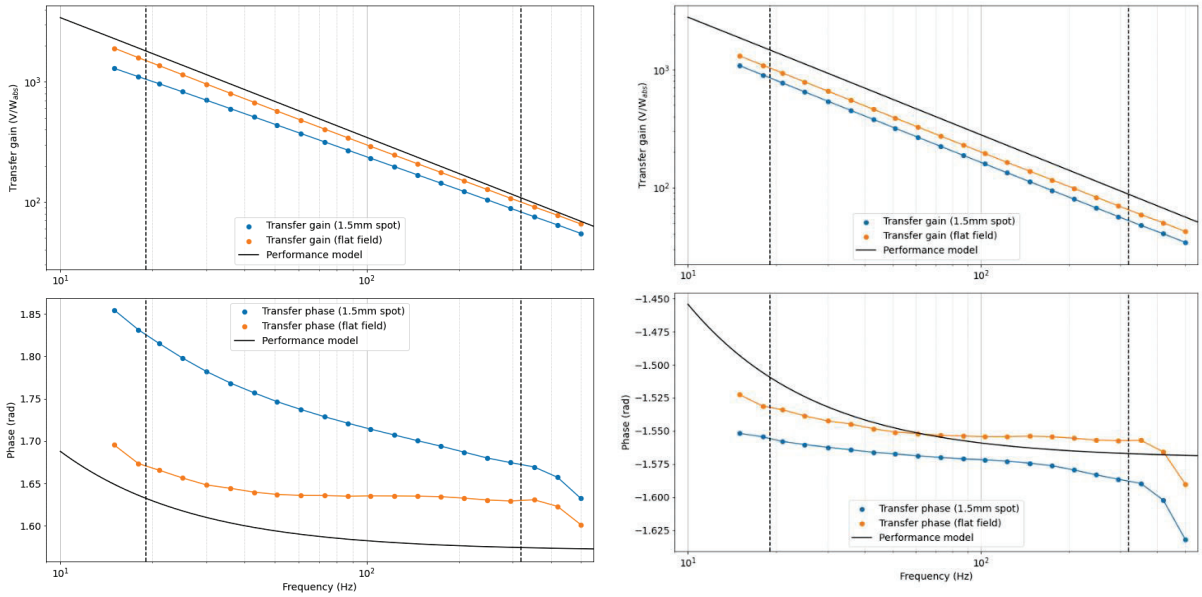

Figure 4-4 Transfer gain amplitude (responsivity) in the upper panes and phase in the lower panes as measured on the P5625 (left) and P5313 (right) detectors with visible light. The data is applicable to absorbed optical power and does thus not contain effects of the optical window or the black coating. The black line is a prediction by the performance model. The dotted vertical lines indicate the FORUM modulation frequency range.

The phase measurements show rather good agreement with the model predictions close to the expected 90° phase shift at frequencies far above the second edge frequency. In case of the P5625 the deviation between spot and flat-field illumination shows a larger frequency dependency for the gain and the phase data. For the P5313 this ratio is almost frequency independent (see Figure 4-5). This is expected as a consequence of localized heat-sinking feature that was observed in the spot scans as well as the additional sensitive area appearing around the nominal 2 mm disc at low frequencies.

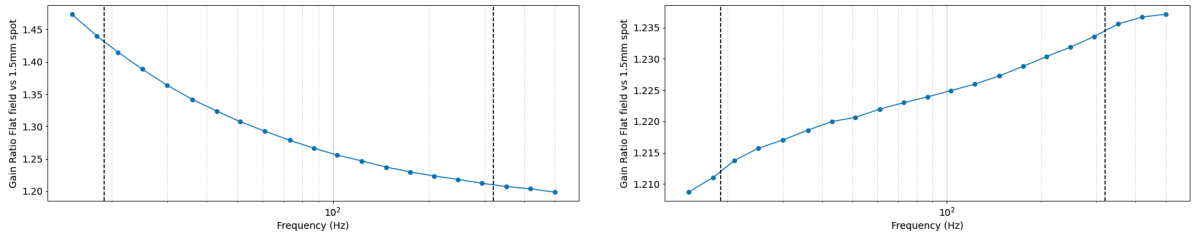

Figure 4-5 Ratio of responsivity as measured in flat-field illumination and the same quantity measured in spot-illumination for the round P5625 detector (left) and the rectangular P5313 detector (right).

Measurements of noise spectral density were performed on the dark P5313 (rectangular, FORUM baseline) detector. The detector together with the proximity electronics of the detection chain was put into a stable thermal enclosure and thermally stabilized at the nominal operating temperature of 23°C. When directly exposed to a laboratory environment with turbulent air flow, the detector picks up a very high level of 1/f noise. A spectrum however shows that typical laboratory induced disturbances are largely limited to below 20 Hz and the FORUM frequency range is almost completely unaffected.

After recording a series of dark data traces, the spectral density of the recorded raw data in LSB/sqrt(Hz) is calculated. This spectrum is corrected for the detection chain transfer function that was measured as part of the GSE commissioning. The resulting detector output noise voltage density is shown in Figure 4-6. The black line indicates the prediction of the performance model. One can see that the characterized detector outperforms the prediction and that the detector noise level is actually very close to the background noise floor of the detection chain breadboard. As discussed above, a significantly improved noise floor is expected on an upcoming design iteration of the detection chain.

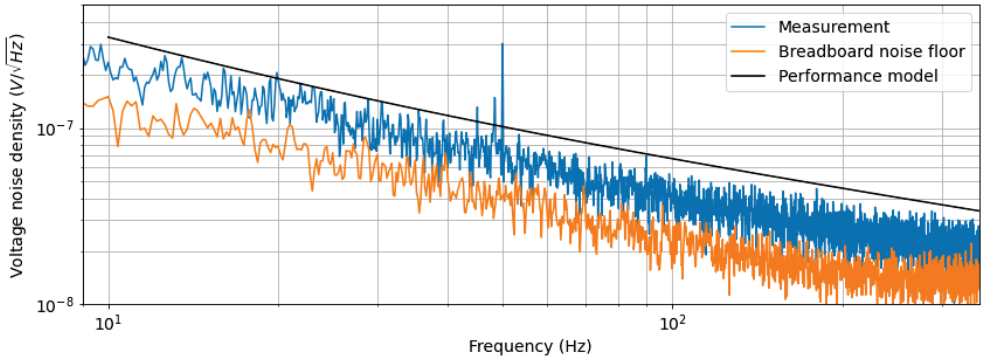

Figure 4-6 Detector output noise voltage density as recorded on P5313. The black line shows the prediction of the performance model.

The detector noise-equivalent power spectral density can be calculated from the transfer gain and the voltage noise spectral density. The detector noise contribution has been extracted from the measured data by taking the square root of the difference of the squared measured noise and the squared detection chain breadboard noise floor. The resulting NEPD values are shown in Figure 4-7. The detector is slightly above the performance prediction at very low frequencies but outperforms the model at higher modulation frequencies.

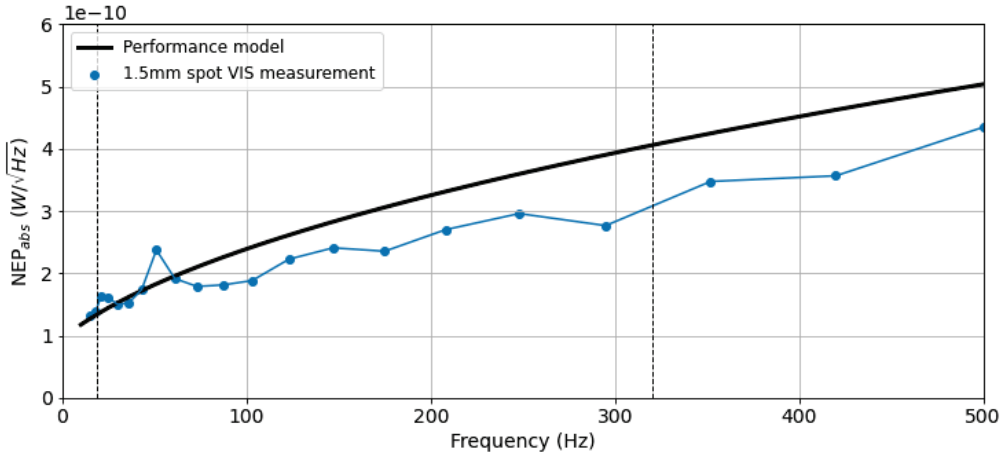

Figure 4-7 Noise-equivalent absorbed optical power spectral density (NEPD) as measured on the rectangular P5313 detector using spot illumination that is representative of the FORUM use case. The black line indicates the performance model prediction and the vertical dashed lines indicate the FORUM modulation frequency range.

Acoustic Susceptibility

Pyroelectric detectors are necessarily also piezoelectric. As such they can act as microphones and import acoustic vibrations directly into the electrical output signal. There, signals caused by acoustics are indiscriminable from signals caused by actual light input and can cause false results. Although no sound exists in the vacuum of space, vibrations that travel along the structures of spacecraft and instrument can cause the same effect. Typical sources are e.g. the momentum wheels in the satellite platform. To quantify the effect, a measurement of acoustic susceptibility has been done on the P5313 detector. The detector was installed on the proximity electronics of the detection chain breadboard and rigidly mounted within an attached metal spider structure. The complete setup was mounted onto a shaker and single-frequency excitations and sine sweeps at 250 mg peak acceleration were run in the in-plane and out-of-plane orientation of the detector sensitive area. As a consistency check, the detector was also held in close vicinity of the operating shaker with no direct mechanical contact. This was done to exclude that observed signals were in fact caused by EMC couplings between the shaker and the detection chain.

A sweep between 10 Hz and 2 kHz was executed with 4 octaves/min. A raw data trace recorded during the out-of-plane sweep is shown in Figure 4-8. The data contains high-amplitude signals at low frequencies as expected from turbulent air in the laboratory and changing ambient conditions. During the shaker measurements, people were standing next to and moving in front of the detector. The shaker-induced signal is not visible within the raw data.

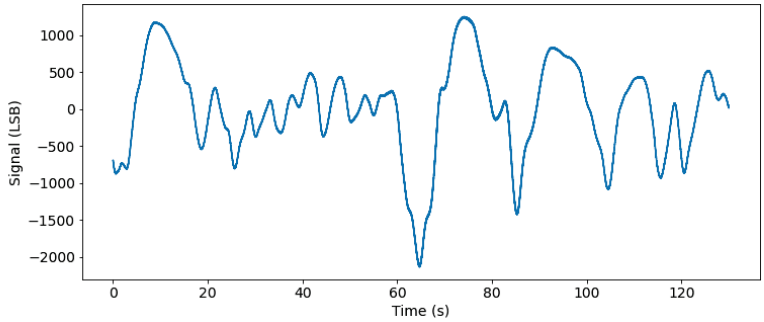

Figure 4-8 Raw data trace recorded during the 250mg sine sweep of the P5313 detector during in the out-of-plane orientation.

The shaker-induced signal however does show up nicely in a short-time Fourier transform (STFT) of the signal (see Figure 4-9). The signal was numerically high-pass filtered with an edge frequency of 5 Hz prior to processing. A spectral

component that grows exponentially with 4 octaves/min is clearly recognizable in the data. The exact point in time when the shaker starts is now known since no active synchronization between shaker run and data recording was done. The red dashed line shows a theoretical model that is fit to the data by maximizing the line integral of the STFT along the theoretical model as a function of the assumed shaker start time. This way, the shaker start time can be extracted very accurately (< 10ms uncertainty). In the next processing step, the sweeped shaker signal with an additional offset of 191 Hz is calculated:

$$a(t) = g_0 * \sin\left(\int_{t_0}^{t} 191 + 10 * 2^{\left(\frac{\tau}{60}*4\right)}\, d\tau\right)$$

This signal is multiplied onto the data to act as a local oscillator. Spectral components that frequency synchronized with the shaker are mixed down to the constant intermediate frequency of 191 Hz. By applying a numeric narrowband filter at 191 Hz, the shaker-induced signal can be extracted from far below the spectrally broad noise floor. The detector output voltage as a function of the frequency is calculated by converting the scan time to frequency using the known shaker sweep and the applying the previously measured detection chain transfer function to convert measured signal at a given frequency to detector output voltage. The acoustic susceptibility is then calculated by dividing the maximum amplitude of the acoustically induced voltage signal by the maximum acceleration of the shaker as recorded by an accelerometer sitting next to the detector under test.

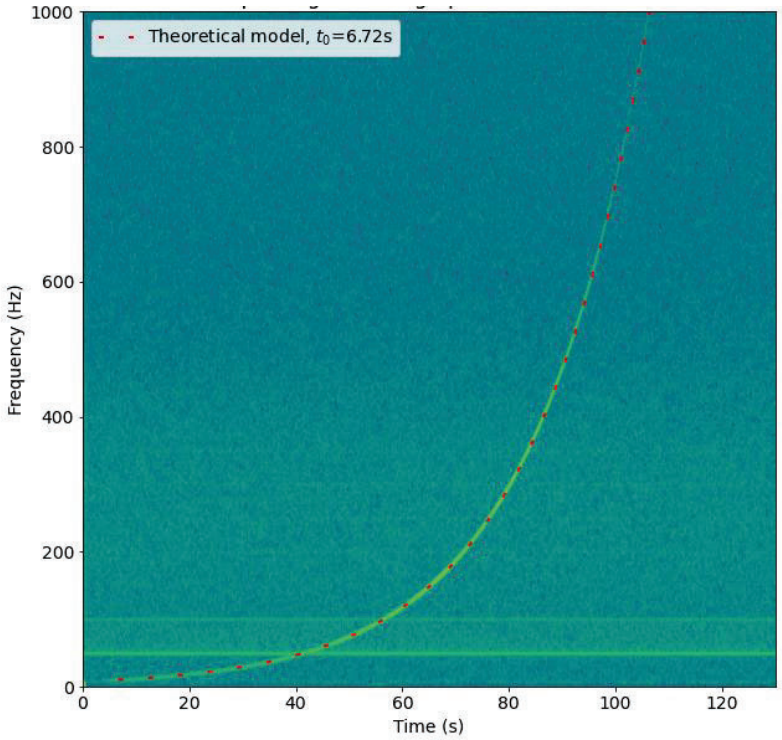

Figure 4-9 Short-time Fourier transform of the raw data recorded on the shaker. The red dashed line indicates the expected spectral positions of shaker-induced signals for a shaker start time of 6.72 s after the start of the pyroelectric data recording.

The resulting measured acoustic susceptibility as measured on the P5313 detector for in-plane and out-of-plane excitation is shown in Figure 4-10. The red dots therein indicate the acoustic susceptibility as evaluated from measurements with CW excitation at a few discrete frequencies. This data was evaluated with a much simpler methodology by narrowband-filtering at the excitation frequency and fitting a sine to the resulting data. It serves as consistency check. The evaluated data agrees well with the values evaluated from the sweep measurements.

Despite two peaks at 180 Hz and 1 kHz in the out-of-plane excited measurement the data does not show much structure. It is expected that this data does not show the 1/f trend of the optical responsivity measurement since the thermal part of

the model is not relevant for the mechanism of acoustic signal generation. The oscillating charge directly deposited on the crystal by the piezoelectric effect is not subject to the thermal low pass and the tested frequencies are far above the electrical cut-off frequency. A flat response is thus expected in the absence of mechanical resonances.

The out-of-plane excitation generally shows about two-fold reduced acoustic susceptibility with an average value of approximately 25 µV/g as opposed to 60µV/g for in-plane excitation. The observed values are quite low. At a modulation frequency of 100 Hz, a sinusoidal vibration with 250 mg peak amplitude would cause a signal that corresponds to a light power of 75 nW.

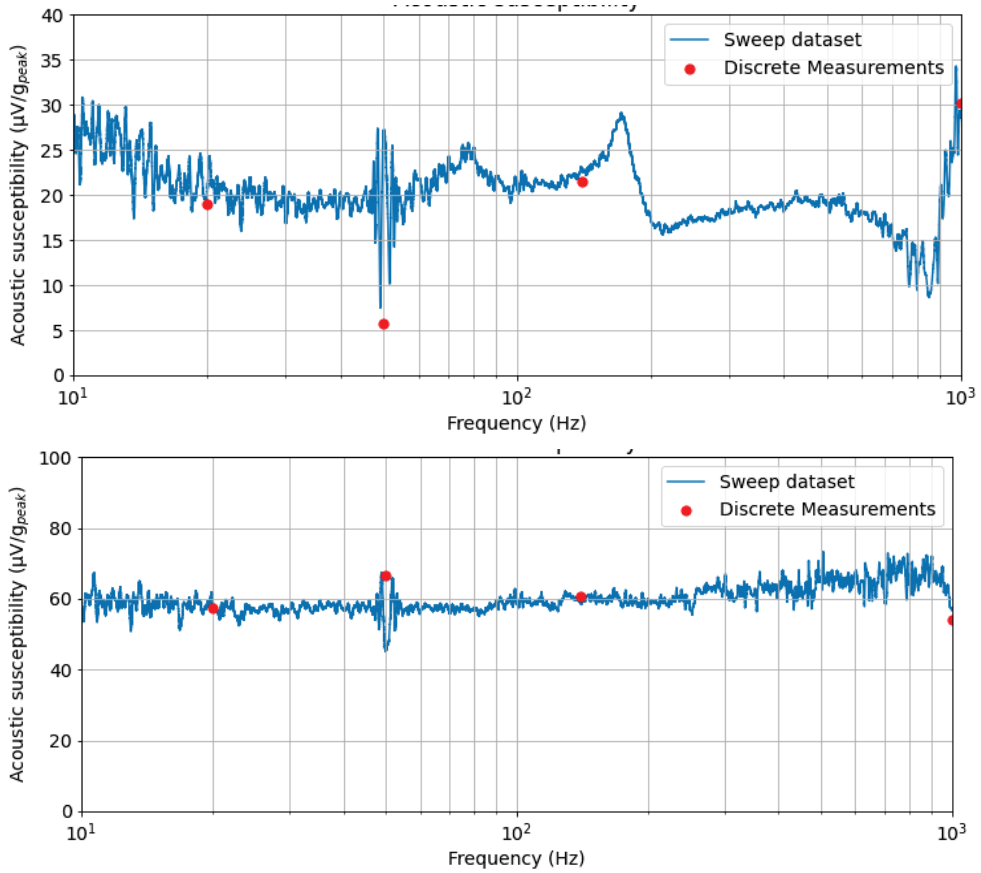

Figure 4-10 Acoustic susceptibility as measured on the P5313 detector for out-of-plane excitation (top panel) and in-plane excitation (bottom panel). The red dots show the results of consistency measurements done with CW excitation at discrete frequencies.

The consistency check performed with the detector being held in the vicinity of the active shaker without direct mechanical contact did indeed not show any signal. This excludes that the observed signal were merely an EMC artefact coupled into the detection chain e.g. through strong magnetic fields generated by the shaker.

5. SUMMARY AND OUTLOOK

This paper presented a series of measurements that were done on two Series 106 detectors provided by *Leonardo UK* in the context of a detector breadboarding campaign at *Airbus Defence and Space Ottobrunn* early in Phase B2 of the FORUM project. A series of optical measurements using a visible light source was performed including spatially resolved maps of responsivity and radiometrically accurate measurements of transfer gain amplitude and phase as a function of light modulation frequency. Further, measurements of acoustic susceptibility done with an active detector mounted to a shaker during a sine sweep were presented.

The major findings of the presented works were:

- The question of how large the sensitive surface is, is surprisingly complex. As a consequence, flat-field illuminated measurements on this type of detector may conclude performance parameters that are not directly applicable to spot-illuminated measurements.
- Towards very low modulation frequencies, the local thermal model of the detector becomes highly relevant. When the penetration depth of the temperature modulation grows beyond the thickness of the crystal, thermal properties of the rear side influence the local responsivity. As a consequence, the round Series 106 detectors show strong local drops in responsivity that appear at low frequencies similar to previously published results on Series 99 detectors.
- The baselined detector according to the P5313 design showed NEP performance that is in good agreement with the Leonardo UK performance model. This is to some extent coincidental as the detector showed lower responsivity than was modelled and measured by Leonardo in flat-field illumination but also lower noise figures.
- The detector was successfully operated on an active shaker and the amplitude of acoustically imported signals could be measured. A final evaluation of the severity of the effects needs to be performed within a system-wide microvibration analysis. The observed susceptibilities however were very low and it is assumed that this will not turn into a problem for the FORUM instrument.

The reported activities were generally very helpful to gain a more thorough understanding of pyroelectric detectors in general and design specifics of the model baselined for FORUM. The results help to identify a clear design baseline and make an educated choice between some subtle design variants that exist within the Leonardo Series 106 COTS detector design.

ACKNOWLEDGMENTS

The detection chain breadboard used to operate the detectors in this study was designed and built by D. Lodie and X. Durand in Airbus Toulouse. The same colleagues also performed initial measurements on the detector during FORUM Phase A/B1 and were available for discussions throughout the reported study.

The work reported in this paper were conducted within the FORUM B2/C/D program funded by the European Space Agency (ESA).

REFERENCES

[1] ESA, “Earth Explorer 9 Candidate Mission FORUM – Report for Mission Selection”, ESA-EOPSM-FORUM-RP-3549 (2019)
[2] Abedin, M., M. Mlynczak and T.F. Refaat, “Infrared detectors overview in the short-wave infrared to far-infrared for the CLARREO mission, SPIE Proceedings 7808 (2010)
[3] A. Rogalski, “Infrared Detectors”, CRC Press (2011)
[4] DIAS Infrared, “Pyroelectric Infrared Detectors”, Application Note (2006)
[5] A. K. Batra, M.D. Aggarwal, “Pyroelectric Materials: Infrared Detectors, Particle Accelerators and Energy Harvesters”, SPIE Press (2013)

[6] S.Y. Wu, “Effects of the Substrate on the Response of Pyroelectric Detectors”, IEEE Transactions on Electron Devices, Vol. ED-27 No. 1 (1980)
[7] K. Domke and A. Odon, “Thermo-electric model of a pyroelectric detector”, WIT Transactions on Engineering Sciences 75, 261-269 (2012)
[8] E. Theocharous, “Absolute linearity measurements on a gold-black-coated deuterated L-alanine doped triglycine sulfate pyroelectric detector”, Applied Optics 47(21), 3731 (2008)